1  Microbial decomposition processes and vulnerable Arctic soil organic carbon in the 21$^{st}$ century

2

3
4  Junrong Zha and Qianlai Zhuang

5

6  Department of Earth, Atmospheric, and Planetary Sciences and Department of Agronomy,
7  Purdue University, West Lafayette, IN 47907 USA

8

10  Correspondence to: qzhuang@purdue.edu

11

12

13

14

15

16

17

18

19

20

21

22

23

24

**Abstract**

**Various levels of representations of biogeochemical processes in current biogeochemistry models contribute to a large uncertainty in carbon budget quantification. Here, we present an uncertainty analysis with a process-based biogeochemistry model, the Terrestrial Ecosystem Model (TEM) that was incorporated with detailed microbial mechanisms. Ensemble regional simulations with the new model (MIC-TEM) estimated the carbon budget of the Arctic ecosystems is 76.0±114.8 Pg C during the 20th century, -3.1±61.7 Pg C under the RCP 2.6 scenario and 94.7±46 Pg C under the RCP 8.5 scenario during the 21st century. Positive values indicate the regional carbon sink while negative values are source to the atmosphere. Compared to the estimates using a simpler soil decomposition algorithm in TEM, the new model estimated that the Arctic terrestrial ecosystems stored 12 Pg less carbon over the 20th century, 19 Pg C and 30 Pg C less under the RCP 8.5 and RCP 2.6 scenarios, respectively, during the 21st century. When soil carbon within depths 30 cm, 100 cm and 300 cm was considered as initial carbon in the 21st century simulations, the region was estimated to accumulate 65.4, 88.6, and 109.8 Pg C, respectively, under the RCP 8.5 scenario. In contrast, under the RCP 2.6 scenario, the region lost 0.7, 2.2, and 3 Pg C, respectively, to the atmosphere. We conclude that the future regional carbon budget evaluation largely depends on whether or not the adequate microbial activities are represented in earth system models and the sizes of soil carbon considered in model simulations.**

47

## 1. Introduction

Northern high-latitude soils and permafrost contain more than 1,600 Pg carbon (Tarnocai et al., 2009). Climate over this region has warmed in recent decades (Serreze and Francis, 2006) and the increase is 1.5 to 4.5 times the global mean (Holland and Bitz, 2003). Warming-induced changes in carbon cycling are expected to exert large feedbacks to the global climate system (Davidson and Janssens, 2006; Christensen and Christensen, 2007; Oechel et al., 2000).

Warming is expected to accelerate soil C loss by increasing soil respiration, but increasing nutrient mineralization, thereby stimulating plant net primary production (NPP) (Mack et al., 2004). Thus, the variation of climate may switch the role of the Arctic system between a C sink and a source if soil C loss overtakes NPP (Davidson et al., 2000; Jobbágy and Jackson, 2000). Process-based biogeochemical models such as TEM (Hayes et al., 2014; Raich and Schlesinger, 1992; McGuire et al., 1992; Zhuang et al., 2001, 2002, 2003, 2010, 2013), Biome-BGC (Running and Coughlan, 1988), CASA (Potter et al., 1993), CENTURY (Parton et al., 1994) and Biosphere Energy Transfer Hydrology scheme (BETHY) (Knorr et al., 2000) have been widely used to quantify the response of carbon dynamics to climatic changes (Todd-Brown et al., 2012). An ensemble of process-based model simulations suggests that arctic ecosystems acted as a sink of atmospheric $CO_2$ in recent decades (McGuire et al., 2012; Schimel et al., 2013). However, the response of this sink to increasing levels of atmospheric $CO_2$ and climate change is still uncertain (Todd-Brown et al., 2013). The IPCC 5th report also shows that land carbon storage is the largest source of uncertainty in the global carbon budget quantification (Ciais et al., 2013).

69    Much of the uncertainty is also due to the relatively lower levels of representation of

70    ecosystem processes that determine the exchanges of water, energy and C between land

71    ecosystems and the atmosphere (Wieder et al., 2013), and ignorance of some key biogeochemical

72    mechanisms (Schmidt et al., 2011). For example, heterotrophic respiration ($R_H$) is the primary

73    loss pathway for soil organic carbon (Hanson et al., 2000; Bond-Lamberty and Thomson, 2010),

74    and it generally increases with increasing temperature (Davidson and Janssens, 2006) and

75    moisture levels in well-drained soils (Cook and Orchard, 2008). Moreover, this process is closely

76    related to soil nitrogen mineralization that determines soil N availability and affects gross

77    primary production (Hao et al., 2015). To date, most models treated soil decomposition as a

78    first-order decay process, i.e., $CO_2$ respiration is directly proportional to soil organic carbon.

79    However, it is not clear if these models are robust under changing environmental conditions

80    (Lawrence et al., 2011; Schimel and Weintraub, 2003; Barichivich et al., 2013) since they often

81    ignored the effects of changes in biomass and composition of decomposers, while recent

82    empirical studies have shown that microbial abundance and community play a significant role in

83    soil carbon decomposition (Allison and Martiny, 2008). The control that microbial activity and

84    enzymatic kinetics imposed on soil respiration suggests the need for explicit representation of

85    microbial physiology, enzymatic activity, in addition to the direct effects of soil temperature and

86    soil moisture on heterotrophic respiration (Schimel and Weintraub, 2003). Recent

87    mechanistically-based models explicitly incorporated with the microbial dynamics and enzyme

88    kinetics that catalyze soil C decomposition have produced notably different results and a closer

89    match to contemporary observations (Wieder et al., 2013; Allison et al., 2010) indicating the need

90    for incorporating these microbial mechanisms into large-scale earth system models to quantify

91    carbon dynamics under future climatic conditions ((Wieder et al., 2013; Allison et al., 2010).

92           This study advanced a microbe-based biogeochemistry model (MIC-TEM) based on an

93    extant Terrestrial Ecosystem Model (TEM) (Raich and Schlesinger, 1992; McGuire et al., 1992;

94    Zhuang et al., 2001, 2002, 2003, 2010, 2013; Hao et al., 2015). In MIC-TEM, the heterotrophic

95    respiration is not only a function of soil temperature, soil organic matter (SOM) and soil

96    moisture, but also considers the effects of dynamics of microbial biomass and enzyme kinetics

97    (Allison et al., 2010). The verified MIC-TEM was used to quantify the regional carbon dynamics

98    in northern high latitudes (north 45 °N) during the $20^{th}$ and $21^{st}$ centuries.

99

100   **2.  Methods**

101   **2.1 Overview**

102   Below we first briefly describe how we advanced the MIC-TEM by modifying the soil

103   respiration process in TEM (Zhuang et al., 2003) to better represent carbon dynamics in

104   terrestrial ecosystems. Second, we describe how we parameterized and verified the new model

105   using observed net ecosystem exchange data at representative sites and how simulated net

106   primary productivity (NPP) was evaluated with Moderate Resolution Imaging Spectroradiometer

107   (MODIS) data to demonstrate the reliability of new model at regional scales. Third, we present

108   how we applied the model to the northern high latitudes for the $20^{th}$ and $21^{st}$ centuries. Finally,

109   we introduce how we conducted the sensitivity analysis on initial soil carbon input, using

110   gridded observation-based soil carbon data of three soil depths during the $21^{st}$ century.

111

**2.2 Model description**

TEM is a highly aggregated large-scale biogeochemical model that estimates the dynamics of carbon and nitrogen fluxes and pool sizes of plants and soils using spatially-explicit information on climate, elevation, soils and vegetation (McGuire et al., 1992; Zhuang et al., 2003, 2010; Melillo et al., 1993). To explicitly consider the effects of microbial dynamics and enzyme kinetics on large-scale carbon dynamics of northern terrestrial ecosystems, we developed MIC-TEM by coupling version 5.0 of TEM (Zhuang et al., 2003, 2010) with a microbial-enzyme module (Hao et al., 2015; Allison et al., 2010). Our modification of the TEM improved the representation of the heterotrophic respiration ($R_H$) from a first-order structure to a more detailed structure (Fig. S1).

In TEM, heterotrophic respiration $R_H$ is calculated as a function of soil organic carbon (SOC), temperature sensitivity of heterotrophic soil respiration ($Q_{10}$), soil moisture (f (MOIST)), and the gram-specific decomposition constant $K_d$:

$$R_H = K_d * SOC * Q_{10}^{\frac{temp}{10}} * f(MOIST) \tag{1}$$

Where temp is soil temperature at top 20 cm (units: ℃). $CO_2$ production from SOC pool is directly proportional to the pool size, and the activity of decomposers only depends on the built-in relationships with soil temperature and moisture (Todd-Brown et al., 2012). Therefore, the changes in microbial community composition or adaption of microbial physiology to new conditions were not represented in TEM. However, current studies indicate that soil C decomposition depends on the activity of biological communities dominated by microbes (Schimel and Weintraub, 2003), implying that the biomass and composition of the decomposer community can't be ignored (Todd-Brown et al., 2012).

134     We thus revised the first-order soil C structure in TEM to a second-order structure

135     considering microbial dynamics and enzyme kinetics according to Allison et al. (2010). In MIC-

136     TEM, heterotrophic respiration ($R_H$) is calculated as:

137                         $$R_H = ASSIM * (1 - CUE)$$                         (2)

138     Where ASSIM and CUE represent microbial assimilation and carbon use efficiency, respectively.

139     ASSIM is modeled with a Michaelis-Menten function:

140                 $$ASSIM = Vmax_{uptake} * MIC * \frac{DOC}{Km_{uptake} + DOC}$$                 (3)

141     Where DOC is dissolved organic carbon and $Vmax_{uptake}$ is the maximum velocity of the

142     reaction and calculated using the Arrhenius equation:

143                 $$Vmax_{uptake} = Vmax_{uptake_0} * e^{-\frac{Ea_{uptake}}{R*(temp+273)}}$$                 (4)

144     Where $Vmax_{uptake_0}$ is the pre-exponential coefficient, $Ea_{uptake}$ is the activation energy for the

145     reaction ($Jmol^{-1}$), R is the gas constant (8.314 $Jmol^{-1}K^{-1}$), and temp is the temperature in Celsius

146     under the reaction occurs. Here we used soil temperature at top 20 cm.

147     Besides, $Km_{uptake}$ is calculated as a linear function of temperature:

148                 $$Km_{uptake} = Km_{uptake_{slope}} * temp + Km_{uptake_0}$$         (5)

149     Microbial biomass MIC is modeled as:

150                 $$\frac{dMIC}{dt} = ASSIM * CUE - DEATH - EPROD$$                 (6)

151     Where microbial biomass death (DEATH) and enzyme production (EPROD) are modeled as

152       proportional to microbial biomass with rate constants $r_{death}$ and $r_{EnzProd}$:

153                         $$DEATH = r_{death} * MIC$$                         (7)

154                         $$EPROD = r_{EnzProd} * MIC$$                         (8)

7

155    Where $r_{death}$ and $r_{EnzProd}$ are the rate constants of microbial death and enzyme production,

156    respectively.

157    DOC is part of soil organic carbon:

158    $$\frac{dDOC}{dt} = DEATH * (1 - MICtoSOC) + DECAY + ELOSS - ASSIM \qquad (9)$$

159    Where MICtoSOC is carbon input ratio as dead microbial biomass to SOC, representing the

160    fraction of microbial death that flows into SOC, and is set as a constant value according to

161    Allison et al. (2010). SOC dynamics are modeled:

162    $$\frac{dSOC}{dt} = Litterfall + DEATH * MICtoSOC - DECAY \qquad (10)$$

163    Where Litterfall is estimated as a function of vegetation carbon (Zhuang et al., 2010). The

164    enzymatic decay of SOC is calculated as:

165    $$DECAY = V_{max} * ENZ * \frac{SOC}{Km + SOC} \qquad (11)$$

166    Where $V_{max}$ is the maximum velocity of the reaction and calculated using the Arrhenius equation:

167    $$V_{max} = Vmax_0 * e^{\frac{Ea}{R*(temp+273)}} \qquad (12)$$

168    The parameters Km and carbon use efficiency (CUE) are temperature sensitive, and calculated

169    as a linear function of temperature between 0 and 50°C:

170    $$Km = Km_{slope} * temp + Km_0 \qquad (13)$$

171    $$CUE = CUE_{slope} * temp + CUE_0 \qquad (14)$$

172    Where $CUE_{slope}$ and $CUE_0$ are parameters for calculating CUE, and $Km_{slope}$ and $Km_0$ are

173    parameters for calculating Km. The values of $CUE_{slope}$, $CUE_0$, $Km_{slope}$, and $Km_0$ were derived

174    from Allison et al. (2010).

175    ELOSS is also a first-order process, representing the loss of enzyme:

176 $$ELOSS = r_{enzloss}*ENZ \qquad\qquad (15)$$

177 Where $r_{enzloss}$ is the rate constant of enzyme loss. Enzyme pool (ENZ) is modeled:

178 $$\frac{dENZ}{dt} = EPROD\text{-}ELOSS \qquad\qquad (16)$$

179       Heterotrophic respiration ($R_H$) is an indispensable component of soil respiration (Bond-

180 Lamberty and Thomson, 2010), and closely coupled with soil nitrogen (N) mineralization that

181 determines soil N availability, affecting gross primary production (GPP).

182

## 2.3 Model parameterization and validation

184 The variables and parameters of these microbial dynamics and their impacts on soil C

185 decomposition were detailed in Allison et al. (2010) (Table 1). Here we parameterized MIC-

186 TEM for representative ecosystem types in northern high latitudes based on monthly net

187 ecosystem production (NEP, $gCm^{-2}$ $mon^{-1}$) measurements from AmeriFlux network (Davidson et

188 al., 2000) (Table S1). The results for model parameterization were presented in Fig. S2. Another

189 set of level 4 gap-filled NEP data was used for model validation at site level (Table S2). The site-

190 level monthly climate data of air temperature (°C), precipitation (mm) and cloudiness (%) were

191 used to drive the model. Gridded MODIS NPP data from 2001 to 2010 were used to evaluate

192 regional NPP simulations. The MODIS NPP data was developed by the MOD17 MODIS project.

193 The product name is Net Primary Production Yearly L4 Global 1 km. The critical parameter used

194 in MOD17 algorithm is conversion efficiency parameter $\mathcal{E}$. More information about the MODIS

195 NPP product can be found at

196 https://neo.sci.gsfc.nasa.gov/view.php?datasetId=MOD17A2_M_PSN.

197 In TEM, NPP is calculated as:

9

198                              NPP=GPP-R$_A$                              (17)

199    Where GPP is gross primary production, and R$_A$ is autotrophic respiration.  GPP is defined as:

200    $$GPP = C_{max} * f(PAR) * f(phenology) * f(foliage) * f(T) * f(CO_2) * f(NA) * f(FT)$$    (18)

201    Where C$_{max}$ is the maximum rate of carbon assimilation, PAR is photosynthetically active

202    radiation, and f(phenology) represents the effects of leaf area (Raich et al., 1991). The function

203    f(foliage) represents the ratio of canopy leaf biomass relative to maximum leaf biomass (Zhuang

204    et al., 2002). T is monthly air temperature, and f(CO$_2$) represents the effects of elevated

205    atmospheric CO$_2$ (McGuire et al., 1997; Pan et al.,1998). The function f(NA) models the limiting

206    effects of plant nitrogen status on GPP (McGuire et al., 1992; Pan et al., 1998). The function f

207    (FT) represents the effects of freeze-thaw (Zhuang et al., 2003). For detailed GPP and R$_A$

208    calculations, see Zhuang et al. (2003).

209    The parameterization was conducted with a global optimization algorithm SCE-UA (Shuffled

210    complex evolution) (Duan et al., 1994) to minimize the difference between the monthly

211    simulated and measured NEE at these sites (Fig. S2). The cost function of the minimization is:

212                    $$Obj = \sum_{i=1}^{k}(NEP_{obs,i}\text{-}NEP_{sim,i})^2$$                    (19)

213    Where NEP$_{obs,i}$ and NEP$_{sim,i}$ are the observed and simulated NEP, respectively. k is the number

214    of data pairs for comparison. Other parameters used in MIC-TEM were default values from TEM

215    5.0 (Zhuang et al., 2003, 2010). The optimized parameters were used for model validation and

216    regional extrapolations.

217

218    **2.4 Regional simulations**

219   Two sets of regional simulations for the 20$^{th}$ century using MIC-TEM and TEM at a spatial

220   resolution of 0.5° latitude $\times$ 0.5° longitude were conducted. Gridded forcing data of monthly air

221   temperature, precipitation, and cloudiness were used, along with other ancillary inputs including

222   historical atmospheric $CO_2$ concentrations, soil texture, elevation, and potential natural

223   vegetation. Climatic inputs vary over time and space, whereas soil texture, elevation, and land

224   cover data are assumed to remain unchanged throughout the 20$^{th}$ century, which only vary

225   spatially. The transient climate data during the 20$^{th}$ century was organized from the Climatic

226   Research Unit (CRU TS3.1) from the University of East Anglia (Harris et al., 2014). The

227   spatially-explicit data include potential natural vegetation (Melillo et al., 1993), soil texture

228   (Zhuang et al., 2003) and elevation (Zhuang et al., 2015).

229   Similarly, two sets of simulations were conducted driven with two contrasting climate

230   change scenarios (RCP 2.6 and RCP 8.5) over the 21$^{st}$ century. The future climate change

231   scenarios were derived from the HadGEM2-ES model, which is a member of CMIP5 project

232   (https://esgf-node.llnl.gov/search/cmip5/). The future atmospheric $CO_2$ concentrations and

233   climate forcing from each of the two climate change scenarios were used. The simulated NPP, $R_H$

234   and NEP by both models (TEM 5.0 and MIC-TEM) were analyzed. The positive NEP represents

235   a $CO_2$ sink from the atmosphere to terrestrial ecosystems, while a negative value represents a

236   source of $CO_2$ from terrestrial ecosystems to the atmosphere.

237   Besides, in order to test the parameter uncertainty in our model, we conducted the

238   regional simulations with 50 sets of parameters for both historical and future studies. The 50 sets

239   of parameters were obtained according to the method in Tang and Zhuang (2008). The upper and

240   lower bounds of the regional estimations were generated based on these simulations.

241

**2.5 Sensitivity to initial soil carbon input**

Future carbon dynamics can be affected by varying initial soil carbon amount. In the standard

simulation of TEM, the initial soil carbon amount for transient simulations was obtained from

equilibrium and spin-up periods directly for each grid cell in the region.  To test the sensitivity to

the initial soil carbon amount in transient simulations for the 21st century, we used empirical soil

organic carbon data extracted from the Northern Circumpolar Soil Carbon Database (NCSCD)

(Tarnocai et al., 2009), as the initial soil carbon amount.  The $0.5° \times 0.5°$ soil carbon data

products for three different depths of 30cm, 100cm and 300cm were used. The sensitivity test

was conducted for transient simulations under the RCP 2.6 and RCP 8.5 scenarios.  To avoid the

instability of C-N ratio caused by replacing the initial soil carbon pool with observed data at the

beginning of transient period, initial soil nitrogen values were also generated based on the soil

carbon data and corresponding C-N ratio map for transient simulations (Zhuang et al., 2003;

Raich and Schlesinger, 1992).

255

**3.  Results**

**3.1 Model verification at site and regional levels**

With the optimized parameters, MIC-TEM reproduces the carbon dynamics well for alpine

tundra, boreal forest, temperate coniferous forest, temperate deciduous forest, grasslands and wet

tundra with $R^2$ ranging from 0.70 for Ivotuk to 0.94 for Bartlett Experimental Forest (Fig. S3,

table S3).  In general, model performs better for forest ecosystems than for tundra ecosystems.

The temporal NPP from 2001 to 2010 simulated by MIC-TEM and TEM were compared with

263 MODIS NPP data (Fig. S4). Pearson correlation coefficients are 0.52 (MIC-TEM and MODIS)

264 and 0.34 (TEM and MODIS). NPP simulated by MIC-TEM showed higher spatial correlation

265 coefficients with MODIS data than TEM (Fig. S5). By considering more detailed microbial

266 activities, the heterotrophic respiration is more adequately simulated using the MIC-TEM. The

267 simulated differences in soil decomposition result in different levels of soil available nitrogen,

268 which influences the nitrogen uptake by plants, the rate of photosynthesis and NPP. The spatial

269 correlation coefficient between NPP simulated by MIC-TEM and MODIS is close to 1 in most

270 study areas, suggesting the reliability of MIC-TEM at the regional scale.

271

272 **3.2 Regional carbon dynamics during the 20th century**

273 The equifinality of the parameters in MIC-TEM was considered in our ensemble regional

274 simulations to measure the parameter uncertainty (Tang and Zhuang, 2008). Here and below, the

275 ensemble means and the inter-simulation standard deviations are shown for uncertainty measure,

276 unless specified as others. These ensemble simulations indicated that the northern high latitudes

277 act from a carbon source of 38.9 Pg C to a carbon sink of 190.8 Pg C by different ensemble

278 members, with the mean of $64.2\pm21.4$ Pg at the end of $20^{th}$ century while the simulation with the

279 optimized parameters estimates a regional carbon sink of 77.6 Pg with the interannual standard

280 deviation of 0.21 Pg C $yr^{-1}$ during the $20^{th}$ century (Fig 1). Simulated regional NEP with

281 optimized parameters using TEM and MIC-TEM showed an increasing trend throughout the $20^{th}$

282 century except a slight decrease during the 1960s (Fig. 2). The Spatial distributions of NEP

283 simulated by MIC-TEM for different periods in the $20^{th}$ century also show the increasing trend

284 (Fig 3). Positive values of NEP represent sinks of $CO_2$ into terrestrial ecosystems, while negative

13

285     values represent sources of $CO_2$ to the atmosphere. From 1900 onwards, both models estimated a

286     regional carbon sink during the 20th century. With optimized parameters, TEM estimated higher

287     NPP and $R_H$ at 0.6 PgC yr$^{-1}$ and 0.3 PgC yr$^{-1}$ than MIC-TEM, respectively, at the end of the 20th

288     century (Fig. 2). The MIC-TEM estimated a carbon sink increase from 0.64 to 0.83 PgCyr$^{-1}$

289     during the century while the estimated increase by TEM was much higher (0.28 PgCyr$^{-1}$) (Fig. 2).

290     At the end of the century, MIC-TEM estimated NEP reached 1.0 PgCyr$^{-1}$ in comparison with

291     TEM estimates of 0.3 PgCyr$^{-1}$. TEM estimated NPP and $R_H$ are 0.5 Pg Cy r$^{-1}$ and 0.3 Pg C yr$^{-1}$

292     higher, respectively. As a result, TEM estimated that the region accumulated 11.4 Pg more

293     carbon than MIC-TEM. Boreal forests are a major carbon sink at 0.55 and 0.63 Pg C yr$^{-1}$

294     estimated by MIC-TEM and TEM, respectively. Alpine tundra contributes the least sink. Overall,

295     TEM overestimated the sink by 12.5% in comparison to MIC-TEM for forest ecosystems and

296     16.7% for grasslands. For wet tundra and alpine tundra, TEM overestimated about 20% and 33%

297     in comparison with MIC-TEM, respectively (Table 2).

298

299     **3.3 Regional carbon dynamics during the 21st century**

300     Simulated regional annual NPP and $R_H$ increases under the RCP 8.5 scenario with both models

301     (Fig. 4). With optimized parameters, MIC-TEM estimated NPP increases from 9.2 in the 2000s

302     to 13.2 PgCyr$^{-1}$ in the 2090s, while TEM-predicted NPP is 2.0 Pg C yr$^{-1}$ higher in the 2000s and

303     0.3 Pg C yr$^{-1}$ higher in the 2090s (Fig. 4). Similarly, TEM also overestimated $R_H$ by 1.7 Pg C yr$^{-1}$

304     in the 2000s and 0.25 Pg C yr$^{-1}$ higher in the 2090s, respectively (Fig. 4). As a result, the regional

305     sink increases from 0.53 Pg C yr$^{-1}$ in the 2000s, 1.4 Pg C yr$^{-1}$ in the 2070s, then decreases to 1.1

306     Pg C yr$^{-1}$ in the 2090s estimated by MIC-TEM (Fig. 4). Given the uncertainty in parameters,

307    MIC-TEM predicted the region acts as a carbon sink ranging from 48.7 to 140.7 Pg, with the

308    mean of 71.7±26.6 Pg at the end of 21$^{st}$ century, while the simulation with optimized parameters

309    estimates a regional carbon source of 79.5 Pg with the interannual standard deviation of 0.37 Pg

310    C yr$^{-1}$ during the 21$^{st}$ century (Fig 4). TEM predicted a similar trend for NEP, which

311    overestimated the carbon sink with magnitude of 19.2 Pg compared with the simulation by MIC-

312    TEM with optimized parameters. Under the RCP 2.6 scenario (Fig. 4), the increase of NPP and

313    R$_H$ is smaller from 2000 to 2100 compared to the simulation under the RCP 8.5. MIC-TEM

314    predicted that NPP increases from 9.1 to 10.9 Pg C yr$^{-1}$, TEM estimated 1.6 Pg C yr$^{-1}$ higher at

315    the beginning and 0.9 Pg C yr$^{-1}$ higher in the end of the 21$^{st}$ century (Fig. 4). Consequently, MIC-

316    TEM predicted NEP fluctuates between sinks and sources during the century, with a neutral

317    before 2070, and a source between -0.2 - -0.3 Pg C yr$^{-1}$ after the 2070s.  As a result, the region

318    acts as a carbon source of 1.6 Pg C with the interannual standard deviation of 0.24 Pg C yr$^{-1}$

319    estimated with MIC-TEM and a sink of 27.6 Pg C with the interannual standard deviation of 0.2

320    Pg C yr$^{-1}$ estimated with TEM during the century (Fig. 4). When considering the uncertainty

321    source of parameters, MIC-TEM predicted the region acts from a carbon source of 64.8 Pg C to a

322    carbon sink of 58.6 Pg C during the century with the mean of -3.3±20.3 Pg at the end of 21$^{st}$

323    century (Fig 4).

324

325    **3.4 Model sensitivity to initial soil carbon**

326    Under the RCP 2.6, without replacing the initial soil carbon with inventory-based estimates

327    (Tarnocai et al., 2009) in model simulations, TEM estimated that the regional soil organic carbon

15

328    (SOC) is 604.2 Pg C and accumulates 12.1 Pg C during the 21st century. When using estimated

329    soil carbon (Tarnocai et al., 2009), within depths of 30cm, 100cm and 300cm as initial pools in

330    simulations, TEM predicted that regional SOC is 429.5, 689.3 and 1003.4 Pg C in 2000, and

331    increases by 9.9, 16.0 and 22.8 Pg C at the end of the 21st century, and the regional cumulative

332    carbon sink is 20.4, 34.0, and 48.1 Pg C, respectively during the century. In contrast, using the

333    same inventory-based SOC estimates, MIC-TEM projected that the region acts from a

334    cumulative carbon sink to a source at 0.7, 2.2, and 3.0 Pg C, respectively. Under the RCP 8.5,

335    both models predicted that the region acts as a carbon sink, regardless of the magnitudes of

336    initial soil carbon pools used, with TEM projected sink of 71.7, 120, and 155.6 Pg C and a much

337    smaller cumulative sink of 65.4, 88.6, and 109.8 Pg C estimated with MIC-TEM, respectively

338    (Table 3).

339    **4. Discussion**

340         During the last few decades, a greening accompanying warming and rising atmospheric

341    $CO_2$ in the northern high latitudes (>45° N) has been documented (McGuire et al., 1995;

342    McGuire and Hobbie, 1997; Chapin and Starfield, 1997; Stow et al., 2004; Callaghan et al., 2005;

343    Tape et al., 2006). The large stocks of carbon contained in the region (Tarnocai et al., 2009) are

344    particularly vulnerable to climate change (Schuur et al., 2008; McGuire et al., 2009). To date, the

345    degree to which the ecosystems may serve as a source or a sink of C in the future are still

346    uncertain (McGuire et al., 2009; Wieder et al., 2013). Therefore, accurate models are essential for

347    predicting carbon–climate feedbacks in the future (Todd-Brown et al., 2013). Our regional

348    simulations indicate the region is currently a carbon sink, which is consistent with many previous

349    studies (White et al., 2000; Houghton et al., 2007), and this sink will grow under the RCP 8.5

350    scenario, but shift to a carbon source under the RCP 2.6 scenario by 2100.  MIC-TEM shows a

351    higher correlation between NPP and soil temperature (R=0.91) than TEM (R=0.82), suggesting

352    that MIC-TEM is more sensitive to environmental changes (Table S4).

353         Our regional estimates of carbon fluxes by MIC-TEM are within the uncertainty range

354    from other existing studies.  For instance, Zhuang et al. (2003) estimated the region as a sink of

355    0.9 Pg C yr$^{-1}$ in extratropical ecosystems for the 1990s, which is similar to our estimation of 0.83

356    Pg C yr$^{-1}$ by MIC-TEM. White et al. (2000) estimated that, during the 1990s, regional NEP

357    above 50 °N region is 0.46 Pg C yr$^{-1}$ while Qian et al. (2010) estimated that NEP increased from

358    0 to 0.3 Pg C yr$^{-1}$ for the high-latitude region above 60 °N during last century, and reached 0.25

359    Pg C yr$^{-1}$ during the 1990s. White et al. (2000) predicted that, from 1850 to 2100, the region

360    accumulated 134 Pg C in terrestrial ecosystems, in comparison with our estimates of 77.6 Pg C

361    with MIC-TEM and 89 Pg C with TEM.  Our projection of a weakening sink during the second

362    half of the 21$^{st}$ century is consistent with previous model studies (Schaphoff et al., 2013). Our

363    predicted trend of NEP is very similar to the finding of White et al. (2000), indicating that NEP

364    increases from 0.46 Pg C yr$^{-1}$ in the 2000s and reaches 1.5 Pg C yr$^{-1}$ in the 2070s, then decreases

365    to 0.6 Pg C yr$^{-1}$ in the 2090s.

366         The MIC-TEM simulated NEP generally agrees with the observations. However, model

367    simulations still deviate from the observed data, especially for tundra ecosystems. The deviation

368    may be due to the uncertainty or errors in the observed data, which do not well constrain the

369    model parameters. Uncertain driving data such as temperature and precipitation are also a source

370    of uncertainty for transient simulations.  In addition, we assumed that vegetation will not change

371    during the transient simulation. However, over the past few decades in the northern high latitudes,

372 temperature increases have led to vegetation changes (Hansen et al., 2006), including latitudinal

373 treeline advance (Lloyd et al., 2005) and increasing shrub density (Sturm et al., 2001). Vegetation

374 can shift from one type to another because of competition for light, N and water (White et al.,

375 2000). For example, needleleaved trees tend to replace tundra gradually in response to warming.

376 In some areas, forests even moved several hundreds of kilometers within 100 years (Gear and

377 Huntley, 1991). The vegetation changes will affect carbon cycling in these ecosystems. In

378 addition, we have not yet considered the effects of management of agriculture lands (Cole et al.,

379 1997), but Zhuang et al. (2003) showed that the changes in agricultural land use in northern high

380 latitudes have been small.

381　　　The largest limitation to this study is that we have not explicitly considered the fire

382 effects. Warming in the northern high latitudes could favor fire in its frequency, intensity,

383 seasonality and extent (Kasischke and Turetsky, 2006; Johnstone and Kasischke, 2005; Soja et al.,

384 2007; Randerson et al., 2006; Bond-Lamberty et al., 2007). Fire has profound effects on northern

385 forest ecosystems, altering the N cycle and water and energy exchanges between the atmosphere

386 and ecosystems. Increase in wildfires will destroy most of above-ground biomass and consume

387 organic soils, resulting in less carbon uptake by vegetation (Harden et al., 2000), leading to a net

388 release of carbon in a short term. However, a suite of biophysical mechanisms of ecosystems

389 including post-fire increase in the surface albedo and rates of biomass accumulation may in turn,

390 exert a negative feedback to climate warming (Amiro et al., 2006; Goetz et al., 2007), further

391 influence the carbon exchanges between ecosystems and the atmosphere.

392　　　Moreover, carbon uptake in land ecosystems depends on new plant growth, which

393 connects tightly with the availability of nutrients such as mineral nitrogen. Recent studies have

394 shown that when soil nitrogen is in short supply, most terrestrial plants would form symbiosis

395 relationships with fungi; hyphae provides nitrogen to plants, in return, plants provide sugar to

396 fungi (Hobbie and Hobbie, 2008, 2006; Schimel and Hättenschwiler, 2007). This symbiosis

397 relationship has not been considered in our current modeling, which may lead to a large

398 uncertainty in our quantification of carbon and nitrogen dynamics.

399     Shift in microbial community structure was not considered in our model, which could

400 affect the temperature sensitivity of heterotrophic respiration (Stone et al., 2012). Michaelis-

401 Menten constant ($K_m$) could also adapt to climate warming, and it may increase more

402 significantly with increasing temperature in cold-adapted enzymes than in warm-adapted

403 enzymes (German et al., 2012; Somero et al., 2004; Dong and Somero, 2009). Carbon use

404 efficiency (CUE) is also a controversial parameter in our model. Empirical studies in soils

405 suggest that microbial CUE declines by at least 0.009 ºC$^{-1}$ (Steinweg et al., 2008), while other

406 studies find that CUE is invariant with temperature (López-Urrutia and Morán, 2007). Another

407 key microbial trait lacking in our modeling is microbial dormancy (He et al., 2015). Dormancy is

408 a common, bet-hedging strategy used by microorganisms when environmental conditions limit

409 their growth and reproduction (Lennon and Jones, 2011). Microorganisms in dormancy are not

410 able to drive biogeochemical processes such as soil $CO_2$ production, and therefore, only active

411 microorganisms should be involved in utilizing substrates in soils (Blagodatskaya and Kuzyakov,

412 2013). Many studies have indicated that soil respiration responses to environmental conditions

413 are more closely associated with the active portion of microbial biomass than total microbial

414 biomass (Hagerty et al., 2014; Schimel and Schaeffer, 2012; Steinweg et al., 2013). Thus, the

415     ignorance of microbial dormancy could fail to distinguish microbes with different physiological

416     states, introducing uncertainties to our carbon estimation.

**5. Conclusions**

418     This study used a more detailed microbial biogeochemistry model to investigate the carbon

419     dynamics in the region for the past and this century. Regional simulations using MIC-TEM

420     indicated that, over the 20th century, the region is a sink of 77.6 Pg C. This sink could reach to

421     79.5 Pg C under the RCP 8.5 scenario or shift to a carbon source of 1.6 Pg under the RCP 2.6

422     scenario during the 21st century. On the other hand, traditional TEM overestimated the carbon

423     sink under the RCP 8.5 scenario with magnitude of 19.2 Pg than MIC-TEM, and predicted this

424     region acting as a carbon sink with magnitude of 27.6 Pg under the RCP 2.6 scenario during the

425     21st century. Using recent soil carbon stock data as initial soil carbon in model simulations, the

426     region was estimated to shift from a carbon sink to a source, with total carbon release at 0.7- 3

427     Pg by 2100 depending on initial soil carbon pools at different soil depths under the RCP 2.6

428     scenario. In contrast, the region acts as a carbon sink at 55.4 - 99.8 Pg in the 21st century under

429     the RCP 8.5 scenario. Without considering more detailed microbial processes, models estimated

430     that the region acts as a carbon sink under both scenarios.  Under the RCP 2.6 scenario, the

431     cumulative sink ranges from 9.9 to 22.8 Pg C.  Under the RCP 8.5 scenario, the cumulative sink

432     is even larger at 71.7 - 155.6 Pg C.  This study indicated that more detailed microbial

433     physiology-based biogeochemistry models estimate carbon dynamics very differently from using

434     a relatively simple microbial decomposition-based model.  The comparison with satellite

435     products or other estimates for the 20th century suggests that the more detailed microbial

436     decomposition shall be considered to adequately quantify C dynamics in northern high latitudes.

447

**References**

449 Allison, S. D., and Martiny, J. B.: Colloquium paper: resistance, resilience, and redundancy in
450 microbial communities, Proceedings of the National Academy of Sciences of the United States
451 of America, 105 Suppl 1, 11512-11519, 10.1073/pnas.0801925105, 2008.
452 Allison, S. D., Wallenstein, M. D., and Bradford, M. A.: Soil-carbon response to warming
453 dependent on microbial physiology, Nature Geoscience, 3, 336-340, 10.1038/ngeo846, 2010.
454 Amiro, B. D., Orchansky, A. L., Barr, A. G., Black, T. A., Chambers, S. D., Chapin Iii, F. S.,
455 Goulden, M. L., Litvak, M., Liu, H. P., McCaughey, J. H., McMillan, A., and Randerson, J. T.:
456 The effect of post-fire stand age on the boreal forest energy balance, Agricultural and Forest
457 Meteorology, 140, 41-50, 10.1016/j.agrformet.2006.02.014, 2006.
458 Barichivich, J., Briffa, K. R., Myneni, R. B., Osborn, T. J., Melvin, T. M., Ciais, P., Piao, S., and
459 Tucker, C.: Large-scale variations in the vegetation growing season and annual cycle of
460 atmospheric CO2 at high northern latitudes from 1950 to 2011, Global change biology, 19, 3167-
461 3183, 10.1111/gcb.12283, 2013.
462 Blagodatskaya, E., and Kuzyakov, Y.: Active microorganisms in soil: Critical review of
463 estimation criteria and approaches, Soil Biology and Biochemistry, 67, 192-211,
464 10.1016/j.soilbio.2013.08.024, 2013.
465 Bond-Lamberty, B., Peckham, S. D., Ahl, D. E., and Gower, S. T.: Fire as the dominant driver of
466 central Canadian boreal forest carbon balance, Nature, 450, 89-92, 10.1038/nature06272, 2007.

467    Bond-Lamberty, B., and Thomson, A.: Temperature-associated increases in the global soil
468    respiration record, Nature, 464, 579-582, 10.1038/nature08930, 2010.
469    Callaghan, T., Björn, L. O., Chernov, Y., Chapin, T., Christensen, T. R., Huntley, B., Ims, R.,
470    Jolly, D., Jonasson, S., Matveyeva, N., Panikov, N., Oechel, W., and Shaver, G.: Arctic tundra
471    and polar desert ecosystems, Arctic climate impact assessment, 243-352, 2005.
472    Chapin, F. S., and Starfield, A. M.: Time lags and novel ecosystems in response to transient
473    climatic change in arctic Alaska, Climatic change, 35, 449-461, 1997.
474    Christensen, J. H., and Christensen, O. B.: A summary of the PRUDENCE model projections of
475    changes in European climate by the end of this century, Climatic Change, 81, 7-30,
476    10.1007/s10584-006-9210-7, 2007.
477    Ciais, P., Sabine, C., Bala, G., Bopp, L., Brovkin, V., Canadell, J., Chhabra, A., DeFries, R.,
478    Galloway, J., Heimann, M., Jones, C., Quéré, C. L., Myneni, R. B., Piao, S., and Thornton, P.:
479    Carbon and other biogeochemical cycles, Climate change 2013: the physical science basis.
480    Contribution of Working Group I to the Fifth Assessment Report of the Intergovernmental Panel
481    on Climate Change, 465-570, 2014.
482    Cole, C. V., Duxbury, J., Freney, J., Heinemeyer, O., K.Minami, Mosier, A., Paustian, K.,
483    Rosenberg, N., Sampson, N., Sauerbeck, D., and Zhao, Q.: Global estimates of potential
484    mitigation of greenhouse gas emissions by agriculture, Nutrient cycling in Agroecosystems, 49,
485    221-228, 1997.
486    Davidson, E. A., Trumbore, S. E., and Amundson, R.: Biogeochemistry: soil warming and
487    organic carbon content, Nature, 408, 2000.
488    Davidson, E. A., and Janssens, I. A.: Temperature sensitivity of soil carbon decomposition and
489    feedbacks to climate change, Nature, 440, 165-173, 10.1038/nature04514, 2006.
490    Dong, Y., and Somero, G. N.: Temperature adaptation of cytosolic malate dehydrogenases of
491    limpets (genus Lottia): differences in stability and function due to minor changes in sequence
492    correlate with biogeographic and vertical distributions, The Journal of experimental biology, 212,
493    169-177, 10.1242/jeb.024505, 2009.
494    Duan, Q., Sorooshian, S., and Gupta, V. K.: Optimal use of the SCE-UA global optimization
495    method for calibrating watershed models, Journal of Hydrology, 158, 265-284, 1994.
496    Esteban G. Jobbágy, and Jackson, R. B.: The vertical distribution of soil organic carbon and its
497    relation to climate and vegetation, Ecological applications, 10, 423-436, 2000.
498    Gear, A. J., and Huntley, B.: Rapid changes in the range limits of Scots pine 4000 years ago,
499    Science, 251, 544-547, 1991.
500    German, D. P., Marcelo, K. R. B., Stone, M. M., and Allison, S. D.: The Michaelis-Menten
501    kinetics of soil extracellular enzymes in response to temperature: a cross-latitudinal study,
502    Global change biology, 18, 1468-1479, 10.1111/j.1365-2486.2011.02615.x, 2012.
503    Goetz, S. J., Mack, M. C., Gurney, K. R., Randerson, J. T., and Houghton, R. A.: Ecosystem
504    responses to recent climate change and fire disturbance at northern high latitudes: observations
505    and model results contrasting northern Eurasia and North America, Environmental Research
506    Letters, 2, 045031, 10.1088/1748-9326/2/4/045031, 2007.
507    Hagerty, S. B., van Groenigen, K. J., Allison, S. D., Hungate, B. A., Schwartz, E., Koch, G. W.,
508    Kolka, R. K., and Dijkstra, P.: Accelerated microbial turnover but constant growth efficiency
509    with warming in soil, Nature Climate Change, 4, 903-906, 10.1038/nclimate2361, 2014.

510 Hansen, J., Sato, M., Ruedy, R., Lo, K., Lea, D. W., and Medina-Elizade, M.: Global
511 temperature change, Proceedings of the National Academy of Sciences of the United States of
512 America, 103, 14288-14293, 10.1073/pnas.0606291103, 2006.
513 Hanson, P. J., Edwards, N. T., Garten, C. T., and Andrews, J. A.: Separating root and soil
514 microbial contributions to soil respiration: A review of methods and observations,
515 Biogeochemistry, 48, 115-146, 2000.
516 Hao, G., Zhuang, Q., Zhu, Q., He, Y., Jin, Z., and Shen, W.: Quantifying microbial
517 ecophysiological effects on the carbon fluxes of forest ecosystems over the conterminous United
518 States, Climatic Change, 133, 695-708, 10.1007/s10584-015-1490-3, 2015.
519 Harden, J. W., Trumbore, S. E., Stocks, B. J., Hirsch, A., Gower, S. T., O'neill, K. P., and
520 Kasischke, E. S.: The role of fire in the boreal carbon budget, Global change biology, 6, 174-184,
521 2000.
522 Harris, I., Jones, P. D., Osborn, T. J., and Lister, D. H.: Updated high-resolution grids of monthly
523 climatic observations - the CRU TS3.10 Dataset, International Journal of Climatology, 34, 623-
524 642, 10.1002/joc.3711, 2014.
525 Hayes, D. J., Kicklighter, D. W., McGuire, A. D., Chen, M., Zhuang, Q., Yuan, F., Melillo, J. M.,
526 and Wullschleger, S. D.: The impacts of recent permafrost thaw on land–atmosphere greenhouse
527 gas exchange, Environmental Research Letters, 9, 045005, 10.1088/1748-9326/9/4/045005, 2014.
528 He, Y., Yang, J., Zhuang, Q., Harden, J. W., McGuire, A. D., Liu, Y., Wang, G., and Gu, L.:
529 Incorporating microbial dormancy dynamics into soil decomposition models to improve
530 quantification of soil carbon dynamics of northern temperate forests, Journal of Geophysical
531 Research: Biogeosciences, 120, 2596-2611, 10.1002/2015jg003130, 2015.
532 Hobbie, E. A., and Hobbie, J. E.: Natural Abundance of 15N in Nitrogen-Limited Forests and
533 Tundra Can Estimate Nitrogen Cycling Through Mycorrhizal Fungi: A Review, Ecosystems, 11,
534 815-830, 10.1007/s10021-008-9159-7, 2008.
535 Hobbie, J. E., and Hobbie, E. A.: 15N in symbiotic fungi and plants estimates nitrogen and
536 carbon flux rates in Arctic tundra, Ecology, 87, 816-822, 2006.
537 Holland, M. M., and Bitz, C. M.: Polar amplification of climate change in coupled models,
538 Climate Dynamics, 21, 221-232, 10.1007/s00382-003-0332-6, 2003.
539 Houghton, R. A.: Balancing the Global Carbon Budget, Annual Review of Earth and Planetary
540 Sciences, 35, 313-347, 10.1146/annurev.earth.35.031306.140057, 2007.
541 Johnstone, J. F., and Kasischke, E. S.: Stand-level effects of soil burn severity on postfire
542 regeneration in a recently burned black spruce forest, Canadian Journal of Forest Research, 35,
543 2151-2163, 10.1139/x05-087, 2005.
544 Kasischke, E. S., and Turetsky, M. R.: Recent changes in the fire regime across the North
545 American boreal region—Spatial and temporal patterns of burning across Canada and Alaska,
546 Geophysical Research Letters, 33, 10.1029/2006gl025677, 2006.
547 Knorr, W.: Annual and interannual CO2 exchanges of the terrestrial biosphere: process-based
548 simulations and uncertainties, Global Ecology and Biogeography, 9, 225-252, 2000.
549 Lawrence, D. M., Oleson, K. W., Flanner, M. G., Thornton, P. E., Swenson, S. C., Lawrence, P.
550 J., Zeng, X., Yang, Z.-L., Levis, S., Sakaguchi, K., Bonan, G. B., and Slater, A. G.:
551 Parameterization improvements and functional and structural advances in Version 4 of the
552 Community Land Model, Journal of Advances in Modeling Earth Systems, 3,
553 10.1029/2011ms000045, 2011.

554 Lennon, J. T., and Jones, S. E.: Microbial seed banks: the ecological and evolutionary
555 implications of dormancy, Nature reviews. Microbiology, 9, 119-130, 10.1038/nrmicro2504,
556 2011.
557 Lloyd, A. H.: Ecological histories from Alaskan tree lines provide insight into future change,
558 Ecology, 86, 1687-1695, 2005.
559 Mack, M. C., Schuur, E. A. G., Bret-Harte, M. S., Shaver, G. R., and III, F. S. C.: Ecosystem
560 carbon storage in arctic tundra reduced by long-term nutrient fertilization, Nature, 431, 2004.
561 McGuire, A. D., Melillo, J. M., Joyce, L. A., Kicklighter, D. W., Grace, A. L., III, B. M., and
562 Vorosmarty, C. J.: Interactions between carbon and nitrogen dynamics in estimating net primary
563 productivity for potential vegetation in North America, Global Biogeochemical Cycles, 6, 101-
564 124, 1992.
565 McGuire, A. D., Melillo, J. M., Kicklighter, D. W., and Joyce, L. A.: Equilibrium responses of
566 soil carbon to climate change: Empirical and process-based estimates, Journal of Biogeography,
567 785-796, 1995.
568 McGuire, A. D., and Hobbie, J. E.: Global climate change and the equilibrium responses of
569 carbon storage in arctic and subarctic regions, In Modeling the Arctic system: A workshop report
570 on the state of modeling in the Arctic System Science program, 53-54, 1997.
571 McGuire, A. D., Anderson, L. G., Christensen, T. R., Dallimore, S., Guo, L., Hayes, D. J.,
572 Heimann, M., Lorenson, T. D., Macdonald, R. W., and Roulet, N.: Sensitivity of the carbon
573 cycle in the Arctic to climate change, Ecological Monographs, 79, 523-555, 2009.
574 McGuire, A. D., Christensen, T. R., Hayes, D., Heroult, A., Euskirchen, E., Kimball, J. S.,
575 Koven, C., Lafleur, P., Miller, P. A., Oechel, W., Peylin, P., Williams, M., and Yi, Y.: An
576 assessment of the carbon balance of Arctic tundra: comparisons among observations, process
577 models, and atmospheric inversions, Biogeosciences, 9, 3185-3204, 10.5194/bg-9-3185-2012,
578 2012.
579 Melillo, J. M., McGuire, A. D., Kicklighter, D. W., III, B. M., Vorosmarty, C. J., and Schloss, A.
580 L.: Global climate change and terrestrial net primary production, Nature, 363, 1993.
581 Oechel, W. C., Vourlitis, G. L., Hastings, S. J., Zulueta, R. C., Hinzman, L., and Kane, D.:
582 Acclimation of ecosystem CO 2 exchange in the Alaskan Arctic in response to decadal climate
583 warming, Nature, 406, 978, 2000.
584 Orchard, V. A., and Cook, F. J.: Relationship between soil respiration and soil moisture, 15, 447-
585 453, 1983.
586 Parton, W. J., Ojima, D. S., Cole, C. V., and Schimel, D. S.: A general model for soil organic
587 matter dynamics: sensitivity to litter chemistry, texture and management, Quantitative modeling
588 of soil forming processes, 147-167, 1994.
589 Potter, C. S., Randerson, J. T., Field, C. B., Matson, P. A., Vitousek, P. M., Mooney, H. A., and
590 Klooster, S. A.: Terrestrial ecosystem production: a process model based on global satellite and
591 surface data, Global Biogeochemical Cycles, 7, 811-841, 1993.
592 Qian, H., Joseph, R., and Zeng, N.: Enhanced terrestrial carbon uptake in the Northern High
593 Latitudes in the 21st century from the Coupled Carbon Cycle Climate Model Intercomparison
594 Project model projections, Global change biology, 16, 641-656, 10.1111/j.1365-
595 2486.2009.01989.x, 2010.
596 Raich, J. W., and Schlesinger, W. H.: The global carbon dioxide flux in soil respiration and its
597 relationship to vegetation and climate, Tellus B, 44, 81-99, 1992.

Randerson, J. T., Liu, H., Flanner, M. G., Chambers, S. D., Jin, Y., Hess, P. G., Pfister, G., Mack, M. C., Treseder, K. K., Welp, L. R., Chapin, F. S., Harden, J. W., Goulden, M. L., Lyons, E., Neff, J. C., Schuur, E. A. G., and Zender, C. S.: The impact of boreal forest fire on climate warming, science, 1130-1132, 2006.

Running, S. W., and Coughlan, J. C.: A general model of forest ecosystem processes for regional applications I. Hydrologic balance, canopy gas exchange and primary production processes., Ecological Modelling, 42, 125-154, 1988.

Schaphoff, S., Heyder, U., Ostberg, S., Gerten, D., Heinke, J., and Lucht, W.: Contribution of permafrost soils to the global carbon budget, Environmental Research Letters, 8, 014026, 10.1088/1748-9326/8/1/014026, 2013.

Schimel, J.: The implications of exoenzyme activity on microbial carbon and nitrogen limitation in soil: a theoretical model, Soil Biology and Biochemistry, 35, 549-563, 10.1016/s0038-0717(03)00015-4, 2003.

Schimel, J.: Microbes and global carbon, Nature Climate Change, 3, 867-868, 10.1038/nclimate2015, 2013.

Schimel, J. P., and Hättenschwiler, S.: Nitrogen transfer between decomposing leaves of different N status, Soil Biology and Biochemistry, 39, 1428-1436, 10.1016/j.soilbio.2006.12.037, 2007.

Schimel, J. P., and Schaeffer, S. M.: Microbial control over carbon cycling in soil, Frontiers in microbiology, 3, 348, 10.3389/fmicb.2012.00348, 2012.

Schmidt, M. W., Torn, M. S., Abiven, S., Dittmar, T., Guggenberger, G., Janssens, I. A., Kleber, M., Kogel-Knabner, I., Lehmann, J., Manning, D. A., Nannipieri, P., Rasse, D. P., Weiner, S., and Trumbore, S. E.: Persistence of soil organic matter as an ecosystem property, Nature, 478, 49-56, 10.1038/nature10386, 2011.

Schuur, E. A. G., Bockheim, J., Canadell, J. G., Euskirchen, E., Field, C. B., Goryachkin, S. V., Hagemann, S., Kuhry, P., Lafleur, P. M., Lee, H., and Mazhitova, G.: Vulnerability of permafrost carbon to climate change: Implications for the global carbon cycle, BioScience, 58, 701-714, 2008.

Serreze, M. C., and Francis, J. A.: The Arctic on the fast track of change, Weather, 61, 65-69, 2006.

Soja, A. J., Tchebakova, N. M., French, N. H. F., Flannigan, M. D., Shugart, H. H., Stocks, B. J., Sukhinin, A. I., Parfenova, E. I., Chapin, F. S., and Stackhouse, P. W.: Climate-induced boreal forest change: Predictions versus current observations, Global and Planetary Change, 56, 274-296, 10.1016/j.gloplacha.2006.07.028, 2007.

Somero, G. N.: Adaptation of enzymes to temperature: searching for basic "strategies", Comparative biochemistry and physiology. Part B, Biochemistry & molecular biology, 139, 321-333, 10.1016/j.cbpc.2004.05.003, 2004.

Steinweg, J. M., Plante, A. F., Conant, R. T., Paul, E. A., and Tanaka, D. L.: Patterns of substrate utilization during long-term incubations at different temperatures, Soil Biology and Biochemistry, 40, 2722-2728, 10.1016/j.soilbio.2008.07.002, 2008.

Steinweg, J. M., Dukes, J. S., Paul, E. A., and Wallenstein, M. D.: Microbial responses to multi-factor climate change: effects on soil enzymes, Frontiers in microbiology, 4, 146, 10.3389/fmicb.2013.00146, 2013.

Stone, M. M., Weiss, M. S., Goodale, C. L., Adams, M. B., Fernandez, I. J., German, D. P., and Allison, S. D.: Temperature sensitivity of soil enzyme kinetics under N-fertilization in two temperate forests, Global change biology, 18, 1173-1184, 10.1111/j.1365-2486.2011.02545.x, 2012.

Stow, D. A., Hope, A., McGuire, D., Verbyla, D., Gamon, J., Huemmrich, F., Houston, S., Racine, C., Sturm, M., Tape, K., Hinzman, L., Yoshikawa, K., Tweedie, C., Noyle, B., Silapaswan, C., Douglas, D., Griffith, B., Jia, G., Epstein, H., Walker, D., Daeschner, S., Petersen, A., Zhou, L., and Myneni, R.: Remote sensing of vegetation and land-cover change in Arctic Tundra Ecosystems, Remote Sensing of Environment, 89, 281-308, 10.1016/j.rse.2003.10.018, 2004.

Sturm, M., Racine, C., and Tape, K.: Climate change: increasing shrub abundance in the Arctic., Nature, 411, 2001.

Tang, J., and Zhuang, Q.: Equifinality in parameterization of process-based biogeochemistry models: A significant uncertainty source to the estimation of regional carbon dynamics, Journal of Geophysical Research: Biogeosciences, 113, 10.1029/2008jg000757, 2008.

Tape, K. E. N., Sturm, M., and Racine, C.: The evidence for shrub expansion in Northern Alaska and the Pan-Arctic, Global change biology, 12, 686-702, 10.1111/j.1365-2486.2006.01128.x, 2006.

Tarnocai, C., Canadell, J. G., Schuur, E. A. G., Kuhry, P., Mazhitova, G., and Zimov, S.: Soil organic carbon pools in the northern circumpolar permafrost region, Global Biogeochemical Cycles, 23, n/a-n/a, 10.1029/2008gb003327, 2009.

Todd-Brown, K. E. O., Hopkins, F. M., Kivlin, S. N., Talbot, J. M., and Allison, S. D.: A framework for representing microbial decomposition in coupled climate models, Biogeochemistry, 109, 19-33, 10.1007/s10533-011-9635-6, 2011.

Todd-Brown, K. E. O., Randerson, J. T., Post, W. M., Hoffman, F. M., Tarnocai, C., Schuur, E. A. G., and Allison, S. D.: Causes of variation in soil carbon simulations from CMIP5 Earth system models and comparison with observations, Biogeosciences, 10, 1717-1736, 10.5194/bg-10-1717-2013, 2013.

White, A., Cannell, M. G. R., and Friend, A. D.: The high-latitude terrestrial carbon sink: a model analysis Global change biology, 6, 227-245, 2000.

Wieder, W. R., Bonan, G. B., and Allison, S. D.: Global soil carbon projections are improved by modelling microbial processes, Nature Climate Change, 3, 909-912, 10.1038/nclimate1951, 2013.

Zhuang, Q., Romanovsky, V. E., and McGuire, A. D.: Incorporation of a permafrost model into a large-scale ecosystem model: Evaluation of temporal and spatial scaling issues in simulating soil thermal dynamics, Journal of Geophysical Research: Atmospheres, 106, 33649-33670, 10.1029/2001jd900151, 2001.

Zhuang, Q., McGuire, A. D., O'Neill, K. P., Harden, J. W., Romanovsky, V. E., and Yarie, J.: Modeling soil thermal and carbon dynamics of a fire chronosequence in interior Alaska, Journal of Geophysical Research, 108, 10.1029/2001jd001244, 2002.

Zhuang, Q., He, J., Lu, Y., Ji, L., Xiao, J., and Luo, T.: Carbon dynamics of terrestrial ecosystems on the Tibetan Plateau during the 20th century: an analysis with a process-based biogeochemical model, Global Ecology and Biogeography, no-no, 10.1111/j.1466-8238.2010.00559.x, 2010.

684 Zhuang, Q., Chen, M., Xu, K., Tang, J., Saikawa, E., Lu, Y., Melillo, J. M., Prinn, R. G., and
685 McGuire, A. D.: Response of global soil consumption of atmospheric methane to changes in
686 atmospheric climate and nitrogen deposition, Global Biogeochemical Cycles, 27, 650-663,
687 10.1002/gbc.20057, 2013.
688 Zhuang, Q., Zhu, X., He, Y., Prigent, C., Melillo, J. M., David McGuire, A., Prinn, R. G., and
689 Kicklighter, D. W.: Influence of changes in wetland inundation extent on net fluxes of carbon
690 dioxide and methane in northern high latitudes from 1993 to 2004, Environmental Research
691 Letters, 10, 095009, 10.1088/1748-9326/10/9/095009, 2015.
692 Zhuang, Q., McGuire, A. D., Melillo, J. M., Clein, J. S., Dargaville, R. J., Kicklighter, D. W.,
693 Myneni, R. B., Dong, J., Romanovsky, V. E., Harden, J., and Hobbie, J. E.: Carbon cycling in
694 extratropical terrestrial ecosystems of the Northern Hemisphere during the 20th century: a
695 modeling analysis of the influences of soil thermal dynamics, Tellus B: Chemical and Physical
696 Meteorology, 55, 751-776, 10.3402/tellusb.v55i3.16368, 2003.
697 Zimov, S. A., Schuur, E. A. G., and III, F. S. C.: Permafrost and the global carbon budget,
698 Science, 312, 1612-1613, 2006.

699

700

701 **Author contributions.** Q.Z. designed the study. J.Z. conducted model development, simulation
702 and analysis. J.Z. and Q. Z. wrote the paper.

703

704 **Competing financial interests.** The submission has no competing financial interests.

705

706 **Materials & Correspondence.** Correspondence and material requests should be addressed to
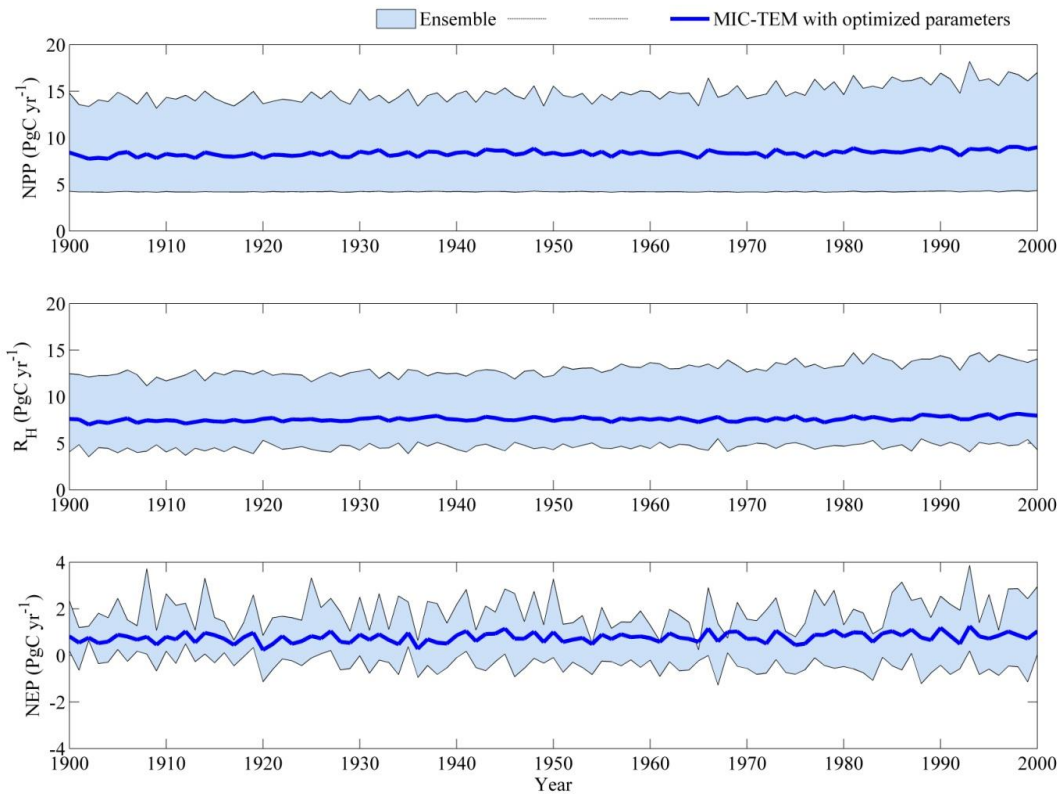707 qzhuang@purdue.edu.

708

709

Figure 1. Simulated annual net primary production (NPP, top panel), heterotrophic respiration ($R_H$, center panel) and net ecosystem production (NEP, bottom panel) by MIC-TEM with ensemble of parameters.
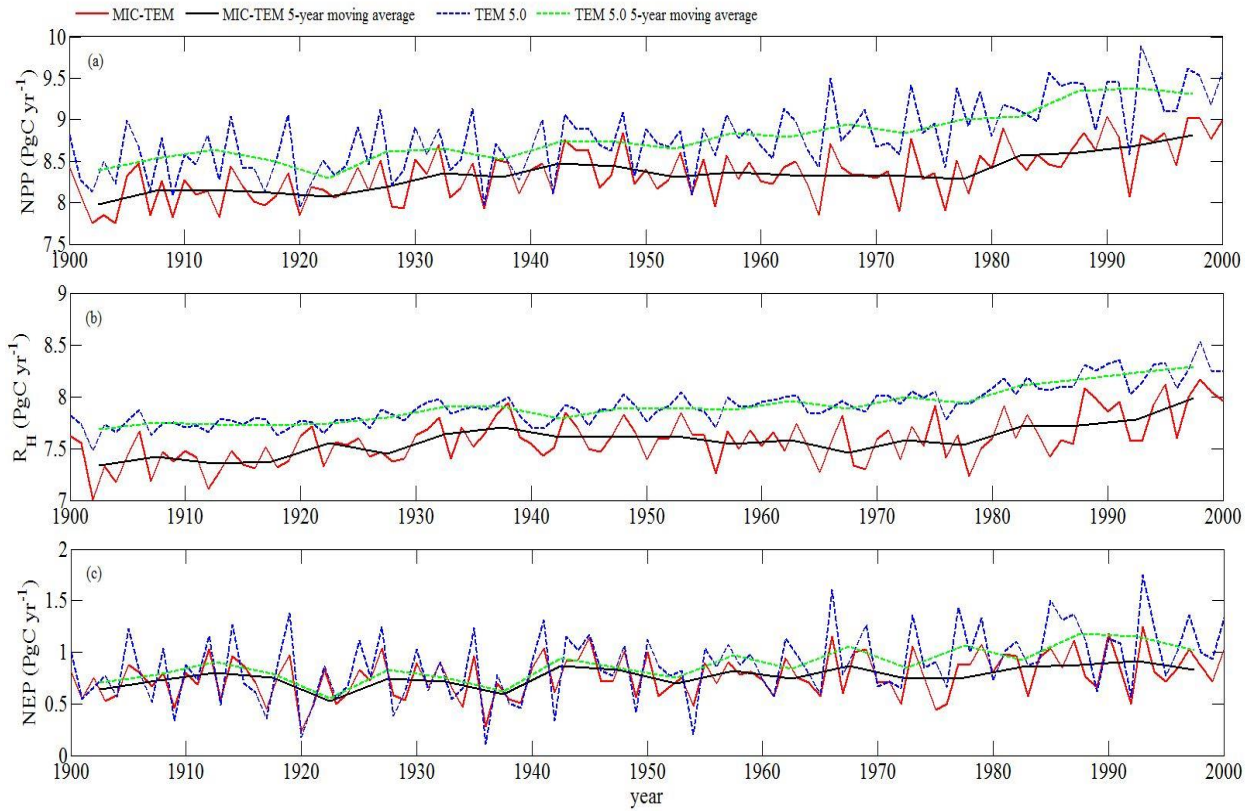
Figure 2. Simulated annual net primary production (NPP, top panel), heterotrophic respiration ($R_H$, center panel) and net ecosystem production (NEP, bottom panel) by MIC-TEM and TEM, respectively.
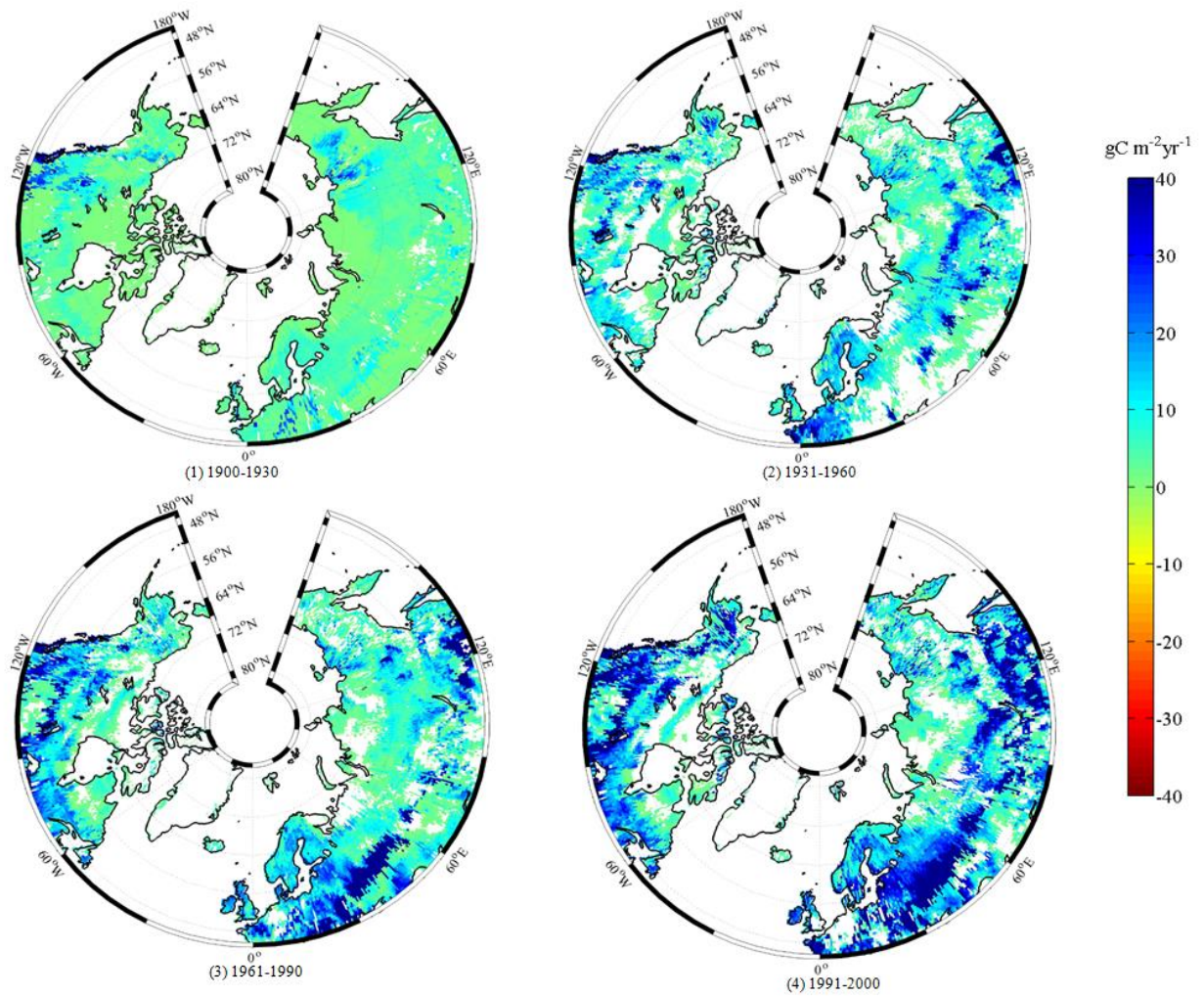
Figure 3. Spatial distribution of NEP simulated by MIC-TEM for the periods: (1) 1900-1930, (2) 1931-1960, (3) 1961-1990, and (4) 1991-2000. Positive values of NEP represent sinks of $CO_2$ into terrestrial ecosystems, while negative values represent sources of $CO_2$ to the atmosphere.
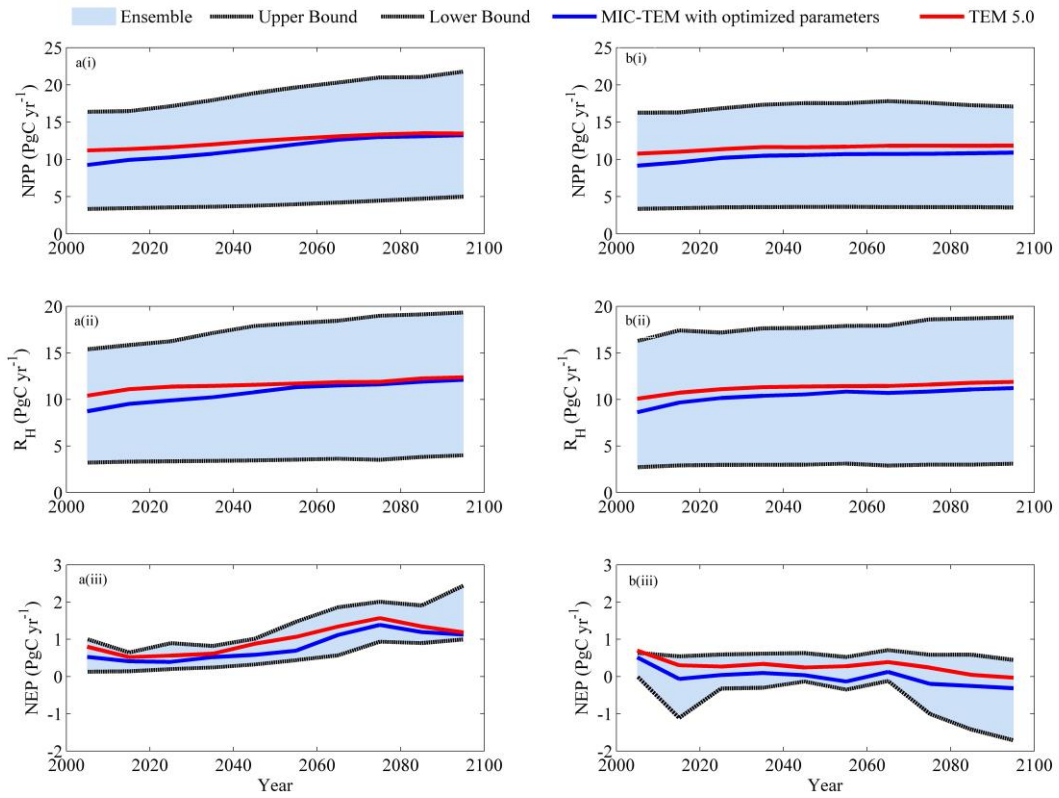
Figure 4. Predicted changes in carbon fluxes: (i) NPP, (ii) $R_H$, and (iii) NEP for all land areas north of 45 °N in response to transient climate change under (a) RCP 8.5 scenario and (b) RCP 2.6 scenario with MIC-TEM and TEM 5.0, respectively. The decadal running mean is applied. The grey area represents the upper and lower bounds of simulations.

**Table 1. Parameters associated with more detailed microbial dynamics in MIC-TEM**

| Process | Parameter | Units | Initial Value | Description | Parameter range | Reference |
|---|---|---|---|---|---|---|
| | $Vmax_{uptake_0}$ | mg DOC cm$^{-3}$ (mg biomass cm$^{-3}$)$^{-1}$ h$^{-1}$ | 9.97e6 | Maximum microbial uptake rate | [1.0e4, 1.0e8] | Hao et al. (2015) |
| | $Ea_{uptake}$ | kJ mol$^{-1}$ | 47 | Activation energy | - | Allison et al. (2010) |
| Assimilation | $Km_{uptake_{slope}}$ | mg cm$^{-3}$ degree$^{-1}$ | 0.01 | Temperature regulator of MM for DOC uptake by microbes | - | Allison et al. (2010) |
| | $Km_{uptake_0}$ | mg cm$^{-3}$ | 0.1 | Temperature regulator of MM for DOC uptake by microbes | - | Allison et al. (2010) |
| | $CUE_{slope}$ | degree$^{-1}$ | -0.016 | Temperature regulator of carbon use efficiency | - | Allison et al. (2010) |
| CO$_2$ production | $CUE_0$ | - | 0.63 | Temperature regulator of carbon use efficiency | - | Allison et al. (2010) |
| | $Vmax_0$ | mg SOC cm$^{-3}$ (mg Enz cm$^{-3}$)$^{-1}$ h$^{-1}$ | 9.17e7 | Maximum rate of converting SOC to soluble C | [1.0e5, 1.0e8] | Hao et al. (2015) |
| Decay | Ea | kJ mol$^{-1}$ | 47 | Activation energy | - | Allison et al. (2010) |
| | $Km_{slope}$ | mg cm$^{-3}$ degree$^{-1}$ | 5 | Temperature regulator of MM for enzymatic decay | - | Allison et al. (2010) |
| | $Km_0$ | mg cm$^{-3}$ | 500 | Temperature regulator of MM for enzymatic decay | - | Allison et al. (2010) |
| | $r_{death}$ | s$^{-1}$ | 0.02 | Microbial death fraction | - | Allison et al. (2010) |
| MIC turnover | MICtoSOC | | 50 | Partition coefficient for dead microbial biomass between the SOC and DOC pool | - | Allison et al. (2010) |
| ENZ turnover | $r_{EnzProd}$ | s$^{-1}$ | 5.0e-4 | Enzyme production fraction | - | Allison et al. (2010) |
| | $r_{EnzLoss}$ | s$^{-1}$ | 0.1 | Enzyme loss fraction | - | Allison et al. (2010) |

**Table 2. Partitioning of average annual net ecosystem production (as Pg C per year) for six vegetation types during the 20th century**

|  | MIC-TEM (PgC yr$^{-1}$) | TEM 5.0 (PgC y$^{-1}$) |
|---|---|---|
| Alpine tundra | 0.03 | 0.04 |
| Boreal forest | 0.39 | 0.45 |
| Conifer forest | 0.09 | 0.09 |
| Deciduous forest | 0.16 | 0.18 |
| Grassland | 0.06 | 0.07 |
| Wet tundra | 0.05 | 0.06 |
| Total | 0.78 | 0.89 |

**Table 3. Increasing of SOC, vegetation carbon (VGC), soil organic nitrogen (SON), vegetation nitrogen (VGN) from 1900 to 2000, and total carbon storage during the 21st century predicted by two models with observed soil carbon data of three different depths under (a) RCP 2.6 and (b) RCP 8.5.**

(a)

| Model | Units: Pg | Without (control) | 30cm | 100cm | 300cm |
|---|---|---|---|---|---|
| | SOC/SON in 2000 | 604.2/27.0 | 429.5/19.0 | 689.3/31.6 | 1003.4/46.2 |
| | Increase of SOC during the 21st century | 12.1 | 9.9 | 16.0 | 22.8 |
| | VGC/VGN in 2000 | 318.3/1.48 | 238.4/1.05 | 394.2/1.80 | 556.7/2.53 |
| TEM 5.0 | Increase of VGC during the 21st century | 15.5 | 10.5 | 18.0 | 25.3 |
| | Increase of total carbon storage during the 21st century | 27.6 | 20.4 | 34.0 | 48.1 |
| | SOC/SON in 2000 | 591.5/26.8 | 420.3/18.6 | 686.0/31.2 | 990.7/45.3 |
| | Increase of SOC during the 21st century | -2.0 | -1.2 | -2.4 | -2.9 |
| | VGC/VGN in 2000 | 309.7/1.42 | 230.1/1.02 | 374.4/1.71 | 548.6/2.45 |
| MIC-TEM | Increase of VGC during the 21st century | 0.4 | 0.5 | 0.2 | -0.1 |
| | Increase of total carbon storage during the 21st century | -1.6 | -0.7 | -2.2 | -3.0 |

(b)

| Model | Units: Pg | Without (control) | 30cm | 100cm | 300cm |
|---|---|---|---|---|---|
| TEM 5.0 | SOC/SON in 2000 | 610.2 /27.9 | 431.9/19.1 | 693.8/31.8 | 1007.1/46.4 |
| | Increase of SOC during the 21$^{st}$ century | 44.2 | 33.0 | 56.5 | 74.6 |
| | VGC/VGN in 2000 | 324.9/1.50 | 242.1/1.07 | 399.6/1.83 | 570.2/2.57 |
| | Increase of VGC during the 21$^{st}$ century | 54.5 | 38.7 | 63.5 | 81.0 |
| | Increase of total carbon storage during the 21$^{st}$ century | 98.7 | 71.7 | 120.0 | 155.6 |
| MIC-TEM | SOC/SON in 2000 | 596.0/27.1 | 424.6/18.8 | 689.1/31.5 | 995.5/46.1 |
| | Increase of SOC during the 21$^{st}$ century | 33.3 | 27.4 | 36.9 | 42.9 |
| | VGC/VGN in 2000 | 316.0/1.44 | 233.5/1.02 | 380.0/1.72 | 568.3/2.56 |
| | Increase of VGC during the 21$^{st}$ century | 46.2 | 37.0 | 51.7 | 56.9 |
| | Increase of total carbon storage during the 21$^{st}$ century | 79.5 | 65.4 | 88.6 | 109.8 |